

An “outside-in” outburst of Aql X–1

T. Shahbaz,¹ R.M. Bandyopadhyay,¹ P.A. Charles,¹ R.M. Wagner,² P. Muhli,³
 P. Hakala,³ J. Casares,⁴ and J. Greenhill⁵

¹University of Oxford, Department of Astrophysics, Nuclear Physics Building, Keble Road, Oxford, OX1 3RH, UK

²Department of Astronomy, Ohio State University, 174 West 18th Ave., Columbus, OH 43210-1106, USA

³Observatory, P.O. Box 14, FIN-00014 University of Helsinki, Finland

⁴Instituto de Astrofísica de Canarias, 38200 La Laguna, Tenerife, Spain

⁵Physics Department, University of Tasmania, GPO Box 252C, Hobart, Tasmania, Australia

arXiv:astro-ph/9807071v1 8 Jul 1998

18 November 2018

ABSTRACT

We present optical spectroscopy and optical and infrared photometry of the neutron star soft X-ray transient Aql X–1 during its X-ray outburst of August 1997. By modelling the X-ray, optical, and IR light curves, we find a 3 day delay between the IR and X-ray rise times, analogous to the UV-optical delay seen in dwarf novae outbursts and black hole X-ray transients. We interpret this delay as the signature of an “outside-in” outburst, in which a thermal instability in the outer disc propagates inward. This outburst is the first of this type definitively identified in a neutron star X-ray transient.

Key words: X-rays: stars – binaries: close – stars: individual: Aql X–1 – stars: neutron – accretion, accretion discs

1 INTRODUCTION

Aquila X–1(=V1333 Aquilae) is known to undergo regular X-ray and optical outbursts on a timescale of \sim 1 year (Kalogren et al. 1977; Priedhorsky & Terrell 1984; Charles et al. 1980), much more frequently than the other neutron star transient Cen X–4 (McClintock & Remillard 1990). Aql X–1 therefore presents us with regular opportunities to test the models proposed to explain the X-ray outbursts occurring in these low-mass X-ray binary transient systems.

Aql X–1 also exhibits type 1 X-ray bursts (Koyama 1981; Czerny, Czerny & Grindlay 1987), indicating that the compact object is a neutron star. Observations in quiescence have shown that the mass-donating companion is a V=19.2 K1 IV star (Shahbaz, Casares & Charles 1997). The optical counterpart brightens by \sim 2–5 magnitudes during X-ray outbursts, interpreted as reprocessing of radiation in the accretion disc (Thorstensen, Charles & Bowyer 1978; Canizares, McClintock & Grindlay 1980; Charles et al. 1980; van Paradijs et al. 1980).

The RXTE All Sky Monitor recorded an X-ray outburst of Aql X–1 between late January and early March 1997 (Levine & Thomas 1997). By 30 March 1997 Aql X–1 was reported to be optically in quiescence (Illovaiky & Chevalier 1997). Aql X–1 then had another outburst in August 1997 (Charles et al. (1997) reported that it had brightened to V=17.8 on August 7 1997), reaching a maximum level at around V=17.5 (Chevalier & Illovaiky 1997). In this letter

we report on X-ray/optical/infrared photometry of Aql X–1 obtained during the August 1997 outburst.

2 OBSERVATIONS AND DATA REDUCTION

A complete journal of the infrared and optical photometric observations is presented in Table 1.

2.1 Infrared Photometry

2.1.1 Lowell Observatory

We obtained *K*-band images of Aql X–1 over a total of 16 nights in 1997 July and August using the Ohio State Infrared Imager/Spectrometer (DePoy et al. 1993) on the Perkins 1.8-m telescope of the Ohio State and Ohio Wesleyan Universities at Lowell Observatory. The 210 images were taken with the *f*/7 camera which provides a 2'7 field of view at a resolution of 0''.63 pixel^{–1}; the seeing was typically 2''.9.

A standard observing sequence consisted of five consecutive images of 60 seconds for Aql X–1; the position of the object on the array was moved between exposures, so that the group could be median-stacked to produce a sky frame. The images were processed by first running a simple interpolation program to remove bad pixels. A median-combined sky image was then created from the five exposures and subtracted from each image. The frames were then flat-fielded using images of a tungsten lamp on a dome flat. These were

taken with the lamp on and also with the lamp off so that the thermal component could be subtracted from the flat-field.

In order to determine the counts for stars in each image we first mosaiced each group of five images so that we could obtain more accurate photometry. The counts for Aql X-1 and a local standard were then computed using the aperture photometry routine described in Shahbaz, Naylor & Charles (1994) with a 3 pixel radius aperture. The magnitudes of Aql X-1 are given relative to a bright star 25 arcsec West and 4 arcsec South of Aql X-1 (Shahbaz et al. 1998). Typical errors in K were 0.08 mags.

2.1.2 UKIRT

We obtained JHK -band images of Aql X-1 on the 16th and 18th July 1997 using the InSb infrared array IRCAM-3, on the 3.8-m United Kingdom Infrared Telescope atop Mauna Kea, Hawaii. Photometric conditions also allowed the acquisition of UKIRT standard stars. A typical observing sequence consisted of eight consecutive images of 10s for Aql X-1, where the object's position on the array was moved between exposures, so that the group could be median stacked to produce a flat-field frame. The standard reduction procedures were then followed.

The counts for Aql X-1 and a local standard were then computed using the aperture photometry routine described in Shahbaz, Naylor & Charles (1994). The magnitude of the local standard was measured, which then allowed us to determine the apparent JHK magnitude for Aql X-1 in quiescence. We obtained $J=16.59\pm0.02$, $H=16.05\pm0.03$ and $K=15.91\pm0.04$.

We could not determine the colour correction between the UKIRT and Lowell filter systems. Therefore we do not use the UKIRT K -band data in the analysis of the IR light curve of Aql X-1.

2.2 Optical Photometry

2.2.1 Teide Observatory

We obtained photometry on the 80cm telescope IAC80 on the nights of 1997 August 12-16, 20-21 and 30 and 1997 September 11 and 15-16. The frames were acquired with a Thomson chip which has a 7.5×7.5 arcmin 2 field of view and a scale of 0.43 arcsec pixel $^{-1}$. Johnson B and V images were obtained using exposure times of 900s and 600s respectively; the seeing was 0.8-1.5 arcsec. Typical errors were 0.10 and 0.05 mags in B and V respectively.

2.2.2 La Palma

On 1997 August 5-8, UBV images were taken at the 2.6-m Nordic Optical Telescope (NOT) at the Observatorio del Roque de los Muchachos on La Palma; one image was taken in each filter on each of the four nights. We also have one V observation from July 30 as well as R and I observations from August 5 and 6. We used a thinned, coated Loral-Lesser 2000x2000 array with typical exposure times of 120 sec in U , 60 sec in B and 30 sec in V . Typical errors were 0.01 and 0.05 mags in B and V respectively.

Table 1. Log of Optical/IR Photometry

Location	Month	Day	Bands
Lowell	July	16,17,18,19,20,23,24,25,26,31	K
	August	1,12,13,14,20,23	K
UKIRT	July	16, 18	K
	July	30	V
	August	5,6,7,8	U, B, V
La Palma	August	5,6	R, I
Tasmania	August	19, 23	V, I
Teide	August	13,14,15,16,21,22,30	B, V
	September	11,15,16	B, V
	October	9,10	B, V

2.2.3 Tasmania

The observations were made on 1997 August 19 and 23 using the Canopus 1-m telescope of the University of Tasmania at a focal ratio of $f/11$. A ST6 CCD photometer with Cousins V and I filters was used with exposures of 5 and 10 minutes.

All of the optical images have undergone standard CCD reduction, including bias subtraction, flat-fielding, and removal of bad pixels. Aperture photometry was performed on Aql X-1 and a local standard using the ARK 'APPHOT' routine; the apertures used ranged from 3-5 pixels in radius, varying with the different instruments and seeing conditions. Magnitudes of Aql X-1 are given relative to the same bright star used for the IR photometry.

2.3 Optical Spectroscopy

Aql X-1 was observed with the ISIS spectrograph on the 4.2-m William Herschel telescope on the nights of 1997 August 6-7. Two 1000s spectra were obtained covering $\lambda\lambda 4110-4910$ and $\lambda\lambda 5900-6700$ for the blue and red arms respectively. A slit width of 0.8 arcsec was used, which when combined with the 600 line/mm grating resulted in a spectral resolution of 1.1 \AA (FWHM=50 km s $^{-1}$ at H α) for the red arm and 1.1 \AA (FWHM=68 km s $^{-1}$ at H β) for the blue arm.

The bias level was removed from each image using the mean overscan regions and then flat-fielded by using a tungsten lamp. One-dimensional spectra were extracted using the standard optimal extraction routines in the PAMELA reduction package, which weights the pixels along the spatial profile in order to obtain the maximum signal-to-noise ratio (Horne 1986); wavelength calibration was performed using the MOLLY package.

2.4 RXTE Observations

The *RXTE* All-Sky Monitor (ASM) has been operating more or less continuously since 1996 February 21, providing roughly five to ten scans of a given source per day in the 2-12 keV energy range. We obtained the one-day average X-ray data for Aql X-1 from the public archive maintained by the *RXTE* Guest Observers Facility. For further details

Table 2. *URI* Optical Photometry. Typical errors are 0.04, 0.03 and 0.01 mags for *U*, *R* and *I* respectively.

Band	Date ^a	Δmag	Band	Date ^a	Δmag
U	666.4490	-1.23	I	666.4564	1.74
	667.3827	-1.42		667.3865	1.76
	668.3835	-1.40		679.5722	1.48
	669.5969	-1.77		679.5770	1.51
R	666.4548	1.40		683.4890	1.36
	667.3858	1.44		683.4957	1.29

^a HJD - 2,450,000.

about the instrument and the methods used in the ASM data reduction and error calculations, see Levine *et al.* (1996).

3 RESULTS

3.1 The distance

The distance to Aql X-1 can be derived using the apparent *K*-band magnitude and the surface brightness S_K of the companion star (Bailey 1981). Using $V=19.2$ (Thorstensen *et al.* 1978) and allowing for an accretion disc contamination in the range 0–50 per cent and reddening of $E_{B-V}=0.35$ mags (Shahbaz *et al.* 1996), we obtain V_o in the range 18.1–18.9.

Using our UKIRT *K*-band magnitude of $K=15.9$ (section 2.1.2) and assuming no disc contamination in the IR (the disc contamination at 6600Å is only 6 per cent: Shahbaz, Casares & Charles 1997) we find $K_o=15.8$. Given the limits for the intrinsic colour of the secondary star and its surface brightness, $(V-K)_o=2.30\text{--}3.05$ and $S_K=3.58\text{--}3.83$ respectively (Ramseyer 1994), and using a secondary star mass of $0.15 M_\odot$ (by comparison with Cen X-4; Shahbaz, Naylor & Charles 1997), we find distance values of 2.2–2.4 kpc (note that the range quoted is due to the uncertainty in the disc contamination in the *V*-band). We conclude that the distance to Aql X-1 is 2.3 ± 0.1 kpc, which is consistent with the previous distance estimate of 2.5 kpc (Charles *et al.* 1980).

3.2 Optical spectrum

Figure 1 shows the optical outburst spectrum of Aql X-1, which exhibits emission features of H α (EW=5.0±0.5Å), H β (EW=2.8±0.5Å), H γ (EW=4.2±0.5Å), HeII 4686Å (EW=3.3±0.4Å) and the Bowen blend 4640–4650Å (EW=2.0±0.3Å). There is also some evidence for an outflow in the system, presumably arising from an accretion disc wind, as the H β emission line has a P-Cygni type profile, where the blue side of the line profile is absorbed. Finally, the emission lines are single-peaked, suggesting that the binary inclination is low.

3.3 X-ray light curve

The August X-ray outburst light curve of Aql X-1 has three distinct sections (see Fig 2). Initially, the X-rays are constant

while the source is quiescent. The X-rays then rise linearly to maximum; the subsequent decay is also linear. The three boundaries on the curve are the time of the initial rise, the time of maximum, and the end of the decay. Using these three boundaries, we simultaneously fitted the data with a three component model; the resultant parameters are given in Table 2. The secondary maximum feature present ∼22 days after the outburst is also seen in other SXTs (Chen, Shrader, & Livio 1997) and was removed from the fitting procedure. A detailed discussion of the secondary maxima will be presented in Shahbaz, Charles & King (1998).

3.4 Optical/IR light curve

The *V*- and *B*-band light curves of Aql X-1 display three distinct phases (see Fig 2). At first, the optical flux rises linearly. However, instead of peaking at X-ray maximum, the *V* and *B* light curves flatten when the X-rays have reached slightly less than half of the maximum intensity. The optical light curve remains in this plateau state until just after the secondary maximum in the X-ray decay (Shahbaz, Charles & King 1998), at which point both *V* and *B* begin a linear decay. By simultaneously fitting the optical light curves with the three-part X-ray model described above, we determine the slopes of the linear rise and decay, and also the start and end of the plateau region. The four *U*-band observations also show a linear rise similar to that seen in the *B* and *V* light curves. *R* and *I* measurements were also obtained; the *URI* relative magnitudes are given in Table 2.

After an initial period of quiescent observations, the *K*-band light curve shows a linear rise and then a decrease in flux which may or may not be associated with the decay. We only fit the initial rise of the light curve and determine the slope and start of the rise. It is interesting to note that the rate of the increase in brightness is largest in *V* and smallest in *K*. However, since the time coverage is sparse, there is some uncertainty in this conclusion. The fit parameters determined for the *V*, *B*, *K*, and X-ray light curves are listed in Table 2.

Our fits to the light curves show that the time of initial rise is earliest in *K* and latest in X-rays. The beginning of the rise in the X-ray intensity occurred on UT July 31 14.4, 3 days after the initial rise in the *K*-band (UT July 28 12.0). This time-delay is significant at the 98.69 per cent level.

In the middle panel of Fig. 2 we show the hardness ratio (3.0–12.0keV/1.3–3.0keV) of the ASM data, which resembles the “flat topped” optical light curves (*B* and *V*). The unusual shape of the optical light curves, which level off rather than following the soft X-ray light curve to its peak, suggest that the flux may arise instead from reprocessing of the hard X-rays. However, inspection of BATSE, ASM, and optical data of two previous outbursts (1996 June and 1997 February) casts doubt on this hypothesis. During the 1996 June event, BATSE recorded a large increase in hard X-rays, while the ASM light curve showed only a small, erratic increase in soft X-rays. In contrast, the 1997 February event was strong in soft X-rays but was not detected by BATSE. The optical light curves of Aql X-1 from both events, however, were very similar, and neither showed the “flat-topped” behaviour seen in our *V*- and *B*-band data (Garcia 1988). It is therefore unclear why our optical light curves do not appear to show direct reprocessing of the entire X-ray flux.

Table 3. Fitted parameters for the August outburst light curves of Aql X-1.

<i>K</i> -band	Slope of linear rise (mags day ⁻¹)	-0.07 ± 0.05
	Start of initial rise ^a	658.0 ± 1.1
<i>V</i> -band	Slope of linear rise (mags day ⁻¹)	-0.14 ± 0.01
	Slope of linear decay (mags day ⁻¹)	0.07 ± 0.01
	Start of plateau ^a	669.6 ± 0.5
	End of plateau ^a	700.0 ± 1.1
<i>B</i> -band	Slope of linear rise (mags day ⁻¹)	-0.11 ± ^{0.12} _{-0.05}
	Slope of linear decay (mags day ⁻¹)	0.09 ± 0.01
	Start of plateau ^a	669.6 ± 0.5
	End of plateau ^a	701.9 ± 1.6
X-rays	Slope of linear rise (cts s ⁻¹ day ⁻¹)	0.76 ± 0.03
	Start of initial rise	661.0 ± 0.5
	Time at maximum light	683.7 ± 0.3
	Slope of linear decay (cts s ⁻¹ day ⁻¹)	-0.51 ± 0.01

^a HJD - 2,450,000.

Spectral information during the entire outburst would help in determining the origin of the optical flux.

4 THE OBSERVED DELAY

The X-ray delay observed in the outburst of Aql X-1 is analogous to the well known UV delay observed for dwarf novae (Warner 1995, and references therein). For dwarf novae the rise in the UV flux starts about 5-15 hours after the beginning of the optical outburst. In the framework of the standard disc instability model (DIM) one can interpret the UV delay as due to an “outside-in” outburst. According to the DIM (e.g. Cannizzo 1993, and references therein), a thermal instability in the outer disc creates a heating front which propagates inward. This front transforms the disc from a cold (quiescent) state to a hot state. Because the UV flux is mainly emitted close to the white dwarf, one expects a delay in its rise equal to the time it takes the front to travel from the outer disc to the white dwarf. In the DIM, however, the calculated travel time of the front is much shorter than the observed UV delay time (~ 1 day; Pringle, Verbunt & Wade 1986; Cannizzo & Kenyon 1987). Thus, in this standard form the model fails to explain the UV delay.

Two solutions have been proposed in order to rescue the DIM, both of which invoke a central hole in the accretion disc. An inward moving heating front would have to stop at the edge of such a hole; the hole would then fill up on a viscous timescale, which is much longer than the heat front propagation time. Livio & Pringle (1992) suggested a mechanism for creating such a hole involving the magnetic field of a weakly magnetized white dwarf, which can disrupt the inner accretion disc. They showed that such a model can reproduce the UV-delay observed in dwarf novae outbursts. Meyer & Meyer-Hofmeister (1994) proposed a different scheme for quiescent accretion onto a white dwarf that also results in a central hole. They invoke inefficient cooling

in the disc’s upper layers, leading to the formation of a hot corona and ultimately to the evaporation of the inner disc.

Whether a hole is created by magnetic fields or by evaporation, the effect on the outburst of a dwarf novae is similar. When the heating front arrives at the inner edge of the truncated disc it cannot propagate any further; the (surface) density contrast slowly fills up the hole on a viscous timescale, thereby producing the required delay of the UV outburst.

Our photometry suggests that the instability that formed the August 1997 outburst started in the outer regions of the disc and propagated inwards (an “outside-in” event), since the brightening started in the *K*-band first and then later in X-rays. The strength of the magnetic field of the neutron star in Aql X-1 has never been determined from observations, although it is believed to be weak, as inferred from the lack of any detectable pulsed X-ray flux in its persistent emission. It is easily conceivable that a hole could be created in the accretion disc, either by the weak magnetic field of the neutron star or by quiescent X-rays ($L_x \sim 4 \times 10^{32}$ ergs s⁻¹; see Verbunt et al. 1994) evaporating the inner regions of the disc. Therefore, as in the case for dwarf novae, one can reproduce the observed time delay between the start of the optical and X-ray outburst. The fact that Aql X-1 has a binary separation 25 percent larger than typical dwarf novae may explain why the IR-X-ray lag in Aql X-1 is longer than the optical-UV lag in the dwarf novae. Detailed computations would be required to see if the 3-day delay between the IR and X-rays can be explained by the DIM model.

Recently Narayan, McClintock & Yi (1996) have proposed a model for the quiescent state of the black hole transients. In the inner region of this model the flow is advection-dominated, *i.e.* it is hot and optically thin and most of the thermal energy is transported across the event horizon, thereby greatly reducing the observed luminosity for the given accretion rate. This is because at these temperatures the radiative cooling timescale is significantly lower than the infall timescale (Narayan et al 1996). For a neutron star system such as Aql X-1 this energy would eventually be radiated from the neutron star surface. The difference between the black hole and neutron star cases has been cited by Narayan, Garcia & McClintock (1997) as evidence for the nature of the compact object.

The key point for Aql X-1 is that the advection-dominated accretion flow (ADAF) region would in effect act as a “hole” in the middle of the disc, since the standard thin disc would be truncated at the edge of the advection-dominated flow. The inner disc becomes advection-dominated at the end of the *previous* outburst when the accretion rate drops below a certain level. We can then estimate the delay we would expect to see by scaling the delay observed in GRO J1655-40 to that in Aql X-1. The ~ 6 day delay seen in GRO J1655-40 can be modelled as the diffusion of the inner edge of the disc to the black hole, starting at $R_{in} = 2.4 \times 10^{10}$ cm (Hameury et al. 1997). The FWZI of the H α emission profile is ~ 1500 km s⁻¹, so for Aql X-1, $R_{in} = 1.4 \times 10^{10}$ cm. If the diffusion rate is the same, we would expect a delay of ~ 3 days (Garcia 1998); this compares well with the observed time delay between our IR and X-ray light curves.

5 THE PROPELLER EFFECT IN AQL X-1?

We now address the observed X-ray properties of Aql X-1, one of only two neutron star SXTs (the other is Cen X-4) and with a very short outburst recurrence time (typically a year or less). In 1997 outbursts were observed in Aql X-1 in Feb. and Aug., the latter of which has been discussed herein. The former outburst was the subject of a more detailed XTE study by Zhang, Yu & Zhang (1998). In particular, Zhang *et al.* found that the X-ray spectral behaviour (as evidenced by its hardness ratio) of Aql X-1 was constant through the decline until just before it entered quiescence, at which point the spectrum hardened dramatically (see Fig. 3).

Zhang *et al.* interpreted this spectral change in terms of the “propeller” effect. This effect has been proposed by Stella, White & Rosner (1986) to account for the cessation of X-ray emission from rapidly spinning pulsars in Be systems when the mass transfer drops below a certain threshold. This is due to matter entering the rapidly spinning magnetosphere, at which radius the rotation speed exceeds the keplerian speed and hence the matter is ejected rather than accreted. Zhang *et al.* propose that Aql X-1 is a spun-up pulsar with a weak magnetic field which exhibits the propeller effect when the accretion rate is sufficiently low. Note that kHz QPOs have now been clearly seen by Cui *et al.* (1998) during the rising phase of the February 1998 outburst.

If the X-ray light curves and spectral properties of other SXTs are examined carefully (e.g. Chen, Shrader, & Livio 1997), then very similar spectral changes at the same stage are seen in A0620-00, GS 1124-683 and GS 2000+25, all of which are (dynamically) established black hole systems in which this mechanism could **not** take place. We also note that this spectral change occurs somewhat after the secondary maximum in the light curve. This is true of the other systems as well, but the observations are too sparse to demonstrate any systematic effect in this delay. There is some evidence for a secondary maximum in the ASM/PCA light curves at \sim 18 days after the outburst peak. In Fig. 3 we show the X-ray light curves of GS 1124-683 and Aql X-1.

In addition to the propeller effect, we propose that other properties of the SXTs can be called upon to account for the spectral hardening. It occurs late in the outburst, after the secondary maximum, the point at which the outer irradiated regions of the disc have been accreted and so, barring the provision of substantial additional material from the secondary, the rate of accretion will be declining. This will provide an opportunity for the remaining inner disc material to be evaporated by the X-radiation, thereby producing the inner hot, low density region which can lead to an ADAF and hence a spherical flow onto the neutron star with a dramatic change in spectrum (but note that being a neutron star system, the accreted luminosity is of course then radiated as it hits the surface).

6 CONCLUSIONS

We have determined a 3 day delay between the IR and X-ray rise times, analogous to the UV-optical delay seen in dwarf novae outbursts and black hole X-ray transients. We interpret this delay as an “outside-in” outburst, in which a thermal instability in the outer disc propagates inward.

We suggest that an ADAF region was created at the end of the previous outburst. The evidence for this comes from the observed hardening of the X-ray spectrum as the system declined into quiescence, a hardening which is also seen in the black hole soft X-ray transients. This ADAF region would appear as a “hole” in the inner accretion disc, thereby causing the X-ray-IR delay when the system starts its next outburst; the hole is needed in order to explain the observed X-ray – IR delay.

ACKNOWLEDGMENTS

We would like to thank Andy Stephens for assisting with the early stages of the IR data analysis, and Ray Bertram for performing some of the IR observations. We also thank Miquel Serra for supporting the service observations of the IAC80 and Tim Naylor for obtaining the UKIRT images. JC acknowledges support by the Spanish Ministry of Science Grant PB 1995-1132-02-01. The data reduction was carried out on the Oxford Starlink node using the ARK software.

REFERENCES

Bailey J., 1981, MNRAS, 218, 619
 Canizares C.R., McClintock J.E., Grindlay J.E., 1980, ApJ, 236, L55.
 Cannizzo J.K., 1993, in Accretion Disks in Compact Stellar Systems, ed. J.C. Wheeler, Singapore, World Scientific, pg 6
 Cannizzo J.K., Kenyon S.J., 1987, ApJ, 320, 319
 Charles P.A. *et al.*, 1980, ApJ 249, 567.
 Charles P.A., Kuulkers E., Casares J., Hakala P., Muhli P., 1997, IAU Circ. 6714.
 Chen W., Shrader C., Livio M., 1997, ApJ, 491, 312
 Chevalier C., Illovasiky S.A., 1991, A&A 251, L11.
 Cui W., Barret D., Zhang S.N., Chen W., Boirin L., Swank K., 1998, ApJ, in press
 Czerny M., Czerny B., Grindlay J.E., 1987, ApJ 312, 122.
 DePoy, D.L., Atwood, B., Byard, P., Frogel, J., & O’Brien, T. 1993, in SPIE Vol. 1946, Infrared Detectors and Instrumentation, p. 667.
 Garcia M., 1998, private communication.
 Hameury J.-M., Lasota J.-P., McClintock J.E., Narayan R., 1997, ApJ 489, 234.
 Horne K., 1986, PASP 98, 609.
 Kaluzienski L.J., Holt S.S., Boldt E.A., Serlemitsos P.J., 1977, Nature 265, 606
 Illovasiky S.A. & Chevalier C., 1997, IAU Circ. 6638.
 Levine A.M., Bradt H., Cui W., Jernigan J.G., Morgan E.H., Remillard R., Shirey R.E., Smith D.A., 1996, ApJ, 469, L33.
 Levine A.M., Thomas B., 1997, IAU Circ. 6558.
 Livio M., Pringle J., 1992, MNRAS, 259, 23
 Koyama K., 1981, ApJ 247, L27.
 McClintock J.E., Remillard R.A., 1990, ApJ 350, 386.
 Meyer F., Meyer-Hofmeister E., 1994, A&A, 288
 Narayan R., McClintock J.E., Yi I., 1996, ApJ, 457, 821. (NMY96)
 Narayan R., Garcia M.R., McClintock J.E., 1997, ApJ, 478, 79
 Priedhorsky W.C., Terrell J., 1980, ApJ 280, 661.
 Pringle J., Verbunt F., Wade R.A., 1986, MNRAS, 221, 169
 Ramseyer T.F., 1994, ApJ, 425, 243
 Shahbaz T., Naylor T., Charles P.A., 1994, MNRAS, 268, 756
 Shahbaz T., Smale A.P., Naylor T., Charles P.A., van Paradijs J., Hassall B., Callanan P., 1996, MNRAS, 282, 1437
 Shahbaz T., Casares J., Charles P.A., 1997, A&A 326, L5.

Shahbaz T., Naylor T., Charles P.A., 1997, MNRAS, 285, 607
Shahbaz T., Charles P.A., King A.R., 1998, MNRAS, in preparation.
Shahbaz T., Thorstensen J.R., Charles P.A., Sherman N.D., 1998,
MNRAS, in press. (SISSA preprint astro-ph/9801240)
Stella L., White N.E., Rosner R., 1986, ApJ, 308, 669
Thorstensen J., Charles P.A., Bowyer S., 1978, ApJ 220, L131.
van Paradijs J., Verbunt F., van der Linden T., Pederson H.,
Wamsteker W., 1980, ApJ 241, L161.
Verbunt F., Belloni T., Johnston H.M., van der Klis M., Lewin
W.H.G., 1994 A&A, 285, 903
Warner B., 1995, Cataclysmic Variable Stars, Cambridge, Cam-
bridge University Press
Zhang S.N., Yu W., Zhang W., 1998, ApJ, 494, L71

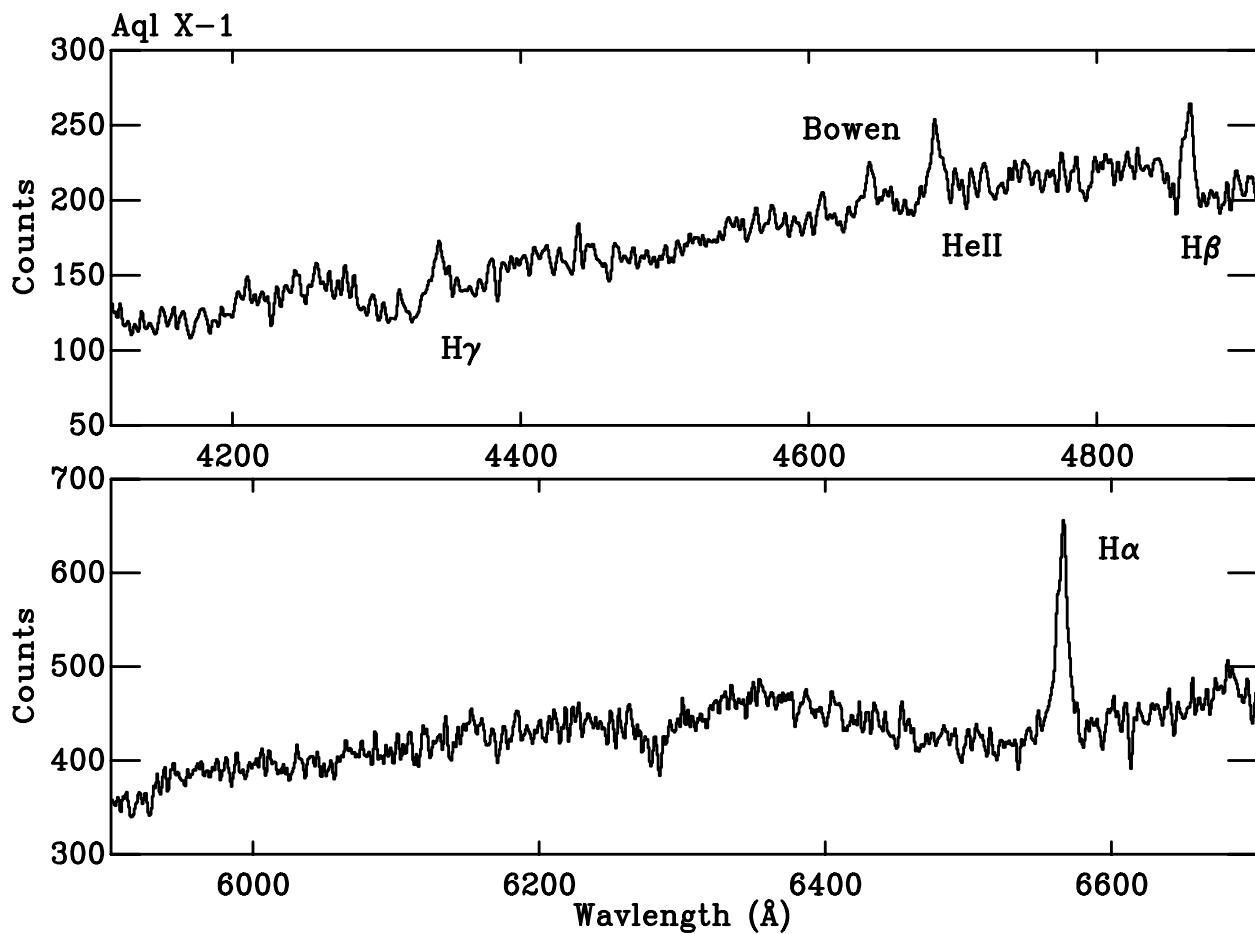


Figure 1. The optical outburst spectrum of Aql X-1. The Balmer (H α , H β and H γ) and HeII (4686 \AA) emission features are present and also the Bowen blend 4640-4650 \AA . The H β emission line has a P-Cygni type profile.

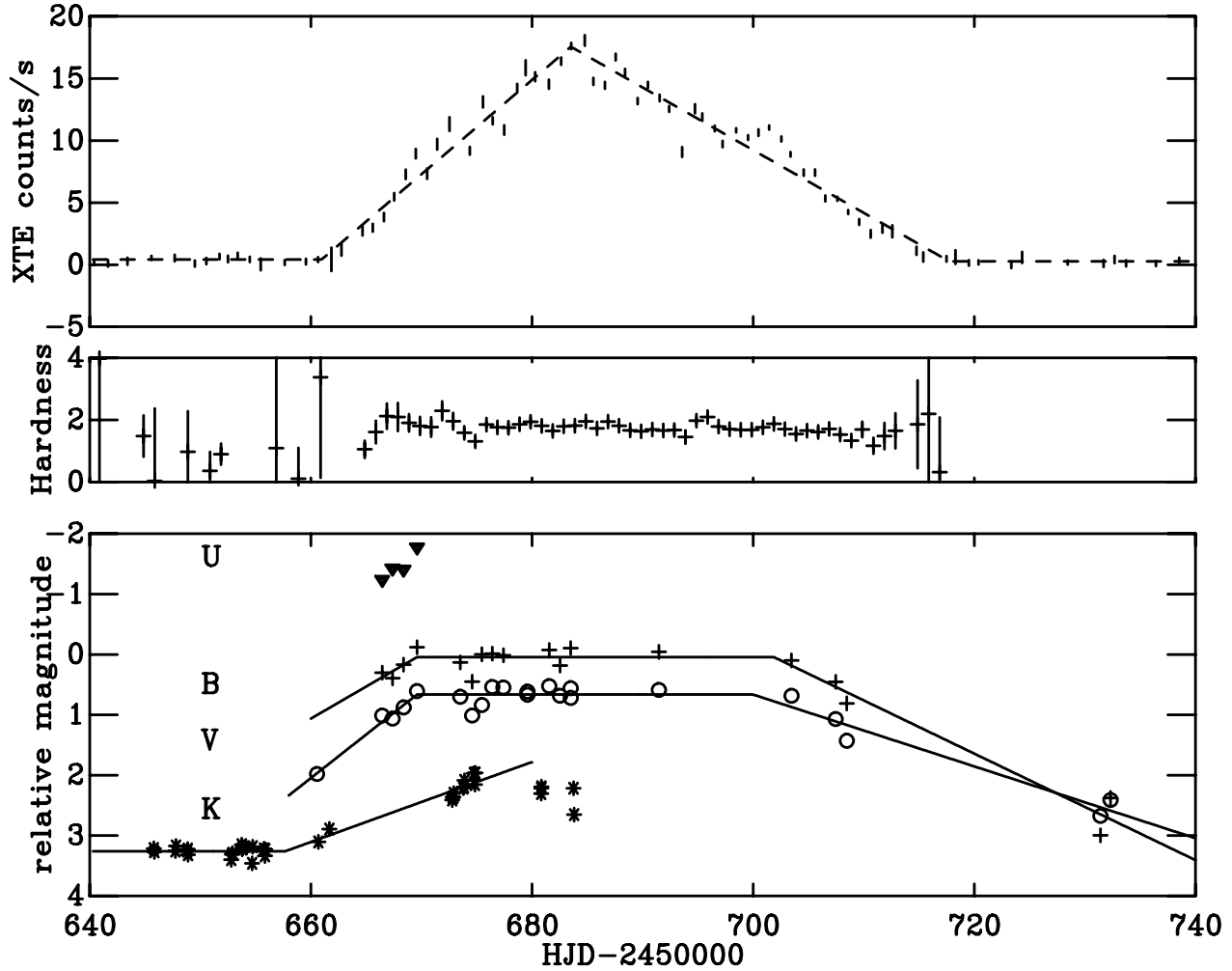


Figure 2. The top panel shows the *RXTE* ASM X-ray light curve (2-12 keV) for the August 1997 outburst of Aql X-1. Also shown is the simultaneous fit to the linear rise and decay. The middle panel shows the ASM hardness ratio (3.0-12.0 keV/1.3-3.0 keV). The bottom panel shows the optical/IR magnitudes of Aql X-1 relative to a local standard (see section 2).

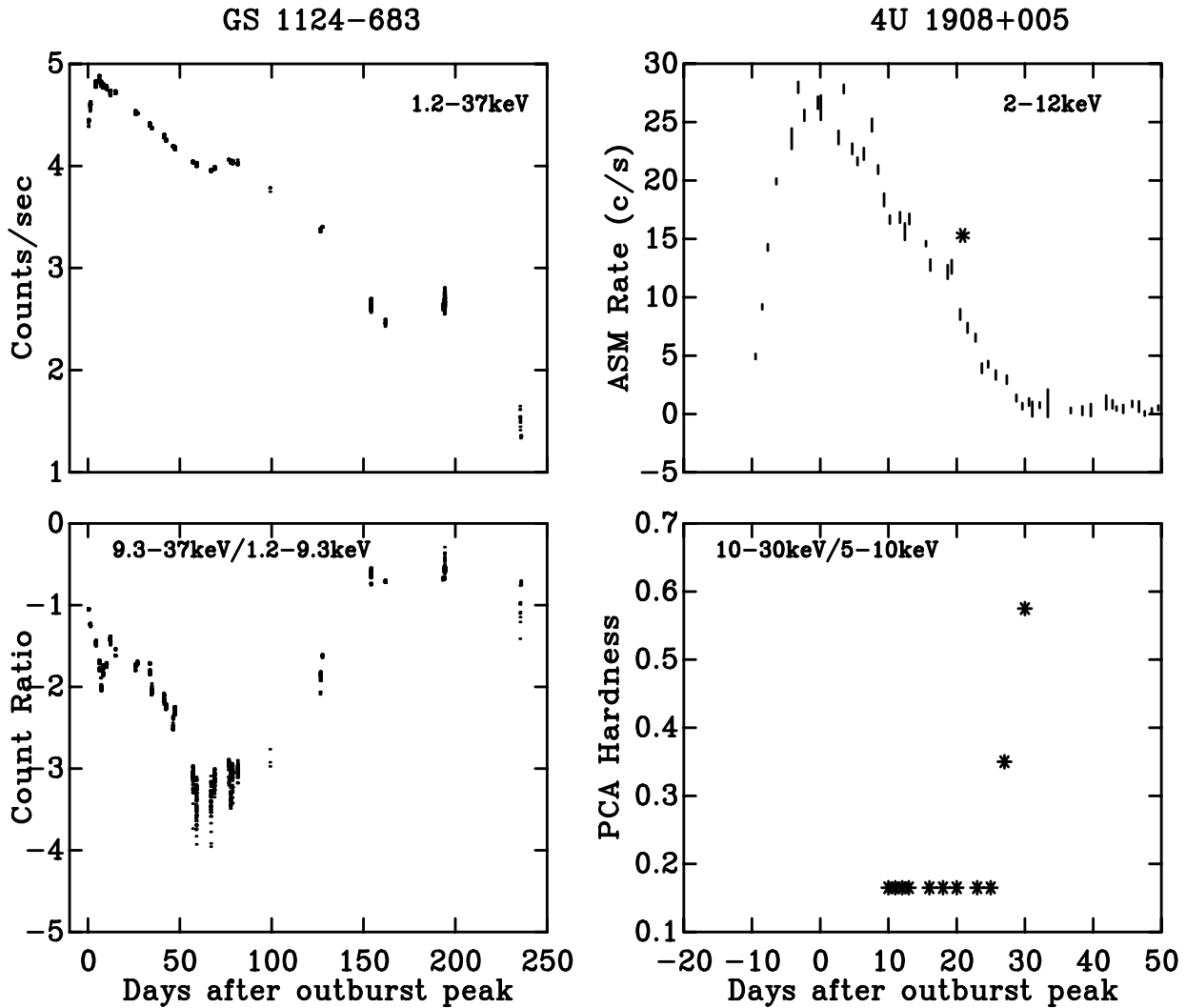


Figure 3. Left figure: The spectral evolution of the January 1991 outburst of GS 1124–68. The top and bottom panel show the LAC (1.2–3.7 keV) count rate and the hardness (9.3–37 keV/1.2–9.3 keV) ratio. Right figure: The spectral evolution of the February 1997 RXTE X-ray outburst of Aql X-1. The top and bottom panel shows the RXTE/ASM (2–12 keV) count rate and PCA hardness (10–30 keV/5–10 keV) ratio. The arrow shows the time at which we expect to see a secondary maximum. Both objects show a clear rise in the hardness ratio after the time of the secondary maximum.